THE ASTROPHYSICAL JOURNAL, 446:L35–L38, 1995 June 10

NEW EVOLUTIONARY TRACKS FOR VERY LOW MASS STARS

I. BARAFFE AND G. CHABRIER
Centre de Recherche Astrophysique de Lyon (UMR CNRS 142), Ecole Normale Supérieure, 69364 Lyon Cedex 07, France
F. ALLARD
Department of Geophysics and Astronomy, University of British Columbia, Vancouver, BC, Canada V6T 1Z4
AND
P. H. HAUSCHILDT
Department of Physics and Astronomy, Arizona State University, Box 871504, Tempe, AZ 85287-1504
Received 1995 January 6; accepted 1995 March 28

ABSTRACT

We present new evolutionary calculations for low-mass and very low mass M dwarfs, for a metallicity range $-2 \leq [M/H] \leq 0$, down to the hydrogen-burning minimum mass ($0.07 < M/M_{\odot} < 0.6$). We use the most recent atmosphere models calculated by Allard & Hauschildt (1995), based on *synthetic* spectra at finite metallicity, and gray atmosphere models based on Alexander & Ferguson (1994) Rosseland opacities.

Comparisons are made with observational results down to the bottom of the main sequence, for different metallicities, in magnitude-color and color-color diagrams. We find excellent agreement between theory and observations over the whole characteristic temperature/luminosity range. This enables us to determine the mass of the faintest objects observed, which is found to be $m_{\rm lim} \approx 0.085\ M_{\odot}$ for [M/H] = 0 and −0.5, and $m_{\rm lim} = 0.09\ M_{\odot}$ for [M/H] = −1.5, for an age of 10 Gyr.

We also examine the effect of the age, the metallicity, and the outer boundary conditions on the evolution.

Subject headings: stars: low-mass, brown dwarfs — stars: evolution — stars: late-type

1. INTRODUCTION

The wealth of observations of very low mass stars (VLMSs) and objects near the bottom of the main sequence has considerably increased over the past few years, and is likely to keep growing within the near future. Present and future observations require the derivation of reliable theoretical models in order to characterize accurately the properties of these objects, i.e., their age, temperature, metallicity, and, above all, their mass, for only the latter property can unambiguously identify a "genuine" brown dwarf.

Many attempts have been made by several groups (D'Antona & Mazzitelli 1985; Burrows, Hubbard, & Lunine 1989; Dorman, Nelson, & Chau 1989; Burrows et al. 1993; Nelson, Rappaport, & Joss 1993) to address this problem. Although the agreement with the observational data improved significantly within the past decade or so, a discrepancy still exists in all these models, which usually predict effective temperatures that are too large for a given luminosity. This stems from the inaccurate treatment of the atmosphere, which in all models relies on *gray* atmospheres. This problem has kept plaguing the theory of VLMs until now and illustrates the limitation of all existing models.

A significant breakthrough was made in the early 1990s by Allard (1990), Kui (1991), and Brett & Plez (1993), who first derived synthetic spectra for temperatures and gravities characteristic of late M dwarfs. Although these calculations yielded a significant improvement in the determination of the effective temperature of VLMSs (Kirkpatrick et al. 1993), some significant discrepancies remained for the coolest, i.e., faintest, objects. A more recent breakthrough is due to the Tucson group (Saumon et al. 1994; Burrows et al. 1993), who first calculated self-consistent *evolutionary models* using synthetic atmosphere models, although these calculations were made for the hypothetical zero-metallicity case.

In this Letter, we present new evolutionary calculations for VLMSs ($0.6 \geq M/M_{\odot} \geq 0.07$), completed with the evolution code developed at the Ecole Normale Supérieure in Lyon. These calculations include the most detailed physics presently available: the equation of state appropriate for dense, low-mass objects (Saumon & Chabrier 1992; Saumon, Chabrier, & Van Horn 1995); improved Rosseland mean opacities (Alexander & Ferguson 1994, hereafter AF94); and the latest generation of synthetic atmosphere models at finite metallicity (Allard & Hauschildt 1995, hereafter AH95). The detailed specification of the various physical ingredients, and the derived mass-luminosity relation and minimum burning masses for light elements, will be presented in a forthcoming paper (Chabrier, Baraffe, & Plez 1995). In this Letter we will focus on the treatment of the atmosphere, i.e., the spectral energy distribution itself (synthetic spectra versus Rosseland means) and the determination of the boundary conditions (gray versus nongray approximation).

2. RESULTS

As shown initially by Allard (1990), for the effective temperature range characteristic of M dwarfs, the energy distribution spectrum *strongly* departs from the blackbody distribution, stressing the need for detailed model atmosphere calculations. Moreover, for most of these effective temperatures and gravities ($\log g \sim 5$), the convection zone penetrates deep into the optically thin outermost layers ($\tau \ll 1$) (Auman 1969; Dorman et al. 1989; Allard 1990; Burrows et al. 1993). This concerns essentially the temperature range 2500 K $\lesssim T_{\rm eff} \lesssim$ 4000 K, which corresponds to H_2 molecular dissociation, yielding a rapid decrease of the adiabatic gradient (see Saumon et al. 1995). Within the aforementioned temperature range, the Eddington approximation or any other prescribed $T(\tau)$ relationship, assuming radiative equilibrium, is no longer valid. The radiative transfer equations, and an appropriate model of convection, must then be solved explicitly.

Recently Allard & Hauschildt (1995) calculated a grid of synthetic atmosphere models which represent a significant improvement over the first-generation models (Allard 1990). This set of models is labeled "Base." In this case, the H_2O and TiO absorption coefficients, a major source of absorption below ~ 3000 K, are calculated within the so-called straight mean approximation. The same authors are currently working on a new set of models, labeled "NextGen," which uses a more complete line-by-line treatment.

As mentioned above, below about 2500 K, the Eddington approximation should become valid again and we can rely on Rosseland opacities. On the other hand, grain formation is found to become substantial, and to dominate the opacity, below $T \sim 1700$ K (AF94). We verified that this process affects only the evolution of objects with a mass $m \leq 0.075\ M_\odot$ at $t = 10$ Gyr and thus concerns essentially the brown dwarf regime. Therefore, grain formation is inconsequential in the *evolution* of VLMSs, but might affect their *spectrum.* Since the "Base" models do not include grain formation, we calculated evolutionary tracks, within the Eddington approximation, with the Rosseland opacities of AF94. Comparison between such gray and nongray models is examined below.

The crucial test for any theoretical model is the comparison with observation! Three years ago, Monet et al. (1992) conducted a trigonometric parallax program which yielded the determination of the photometry (V and I) and the tangential velocity of 72 stars. The data were completed with the parallax determination of the US Naval Observatory photographic program, which added 332 stars to the previous ones. That led to the determination of an observed magnitude-color diagram for VLMSs up to $M_V = 19.37$ and $V-I = 4.7$, thus including the faintest and reddest stellar objects presently observed. More interestingly, the results of Monet et al. show two distinct sequences for the VLMSs, a "red" dwarf sequence ($2 \lesssim V-I \lesssim 4.7$) ending at $M_V \sim 19$, and a "blue" so-called *sub*dwarf sequence ($2 \lesssim V-I \lesssim 3$), which ends up at $M_V \sim 15$. Most of the objects in the dwarf sequence have $V_{\rm tan} < 200$ km s^{-1}, whereas all the identified subdwarfs have $V_{\rm tan} > 200$ km s^{-1}. That strongly suggests that the first sequence displays objects belonging to the disk, i.e., with a *solar-like* metal abundance, whereas the objects of the second sequence are certainly older, halo objects, with *low metallicity.* The sampling in the dwarf sequence has been extended recently by the CCD observations of Kirkpatrick et al. (1993, 1994).

As shown by Monet et al., all the existing theoretical models fail to reproduce the observed magnitude-color diagram for the faintest objects, predicting temperatures that are too large for a given luminosity. For this reason, neither an age nor a mass could be attributed unambiguously to these objects, in particular the faintest ones, believed to lie near the hydrogen-burning minimum mass (HBMM).

Figure 1 shows the comparison between observations and theory for an age $t = 10$ Gyr. A mixing-length parameter $l/H_P = 1$ was used throughout the calculations. Variations of this parameter around this value were found to be inconsequential for the present results. The adopted helium initial mass fraction is $Y = 0.275$. As shown on the figure, the present theoretical models reproduce the observations accurately. That clearly illustrates the particular importance of a proper treatment of the atmosphere, and the necessity of using reliable synthetic spectra, to describe accurately the evolution of VLMSs. Figure 1 highlights the following characteristics:

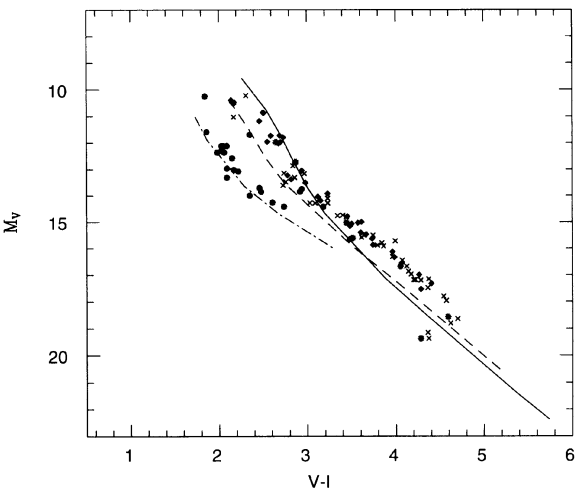

FIG. 1.—Color-magnitude diagram. *Crosses:* Monet et al. (1992) for objects with $V_{\rm tan} < 200$ km s^{-1}; *filled circles:* Monet et al. (1992) for $V_{\rm tan} > 200$ km s^{-1}; *asterisks:* Kirkpatrick et al. (1993); *diamonds:* Kirkpatrick et al. (1994). (For the sake of clarity, only a limited sample is shown.) *Solid line:* [M/H] = 0; *dashed line:* [M/H] = −0.5; *dash-dot line:* [M/H] = −1.5.

1. *Metallicity effect.*—The solid and the dashed curves correspond respectively to [M/H] = 0 (solar composition) and [M/H] = −0.5. Interestingly enough, this spread in metallicity appears only for the more massive, and then more luminous objects, i.e., for $M_V \lesssim 15$, and reflects the observational variation mentioned by Monet et al. (1992). This spread disappears above the aforementioned magnitude, for *both* the observations and the theoretical models, suggesting a real, physical effect rather than a flaw in the models. This magnitude corresponds to $T_{\rm eff} \approx 2800$ K for $t = 10$ Gyr, for which the convection zone reaches out to the region of molecule formation, in particular H_2O, which dominates the opacity in the infrared (H and K bands), and TiO and VO, which dominate in the optical (R, I).

The observed *sub*dwarf sequence is perfectly reproduced for a metallicity [M/H] = −1.5. For [M/H] = −2, the sequence was found to be shifted blueward by ~ 0.2 mag. This validates the mean metallicity of −1.7 adopted by Monet et al. for their extreme subdwarfs.

The present calculations allow the analysis of further different effects. For the sake of clarity, these effects are displayed only for the *dwarf* sequence, and are shown in Figure 2. In all cases, the solid curve corresponds to the complete calculations described previously, with [M/H] = 0 and for $t = 10$ Gyr.

2. *Age effect.*—Figure 2 shows calculations for $t = 10^{10}$ yr (*solid line*) and $t = 10^8$ yr (*dotted line*). Younger objects, still in the pre–main-sequence contraction phase, have a smaller mass for a given luminosity, and then a smaller temperature (see, e.g., D'Antona & Mazzitelli 1994), and are shifted redward (larger $V-I$). The spread in age remains fairly small. For $t = 10^8$ yr,

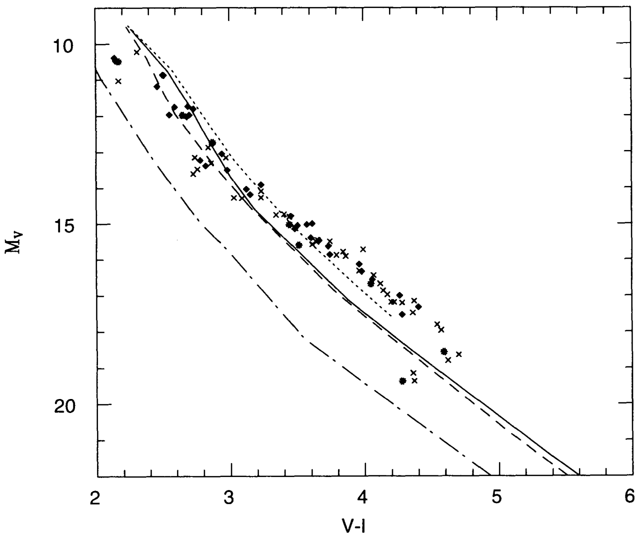

FIG. 2.—Color-magnitude diagram for the dwarf sequence only (same observations as in Fig. 1). Models are represented for [M/H] = 0. *Solid line:* $t = 10^{10}$ yr; *dotted line:* $t = 10^8$ yr; *dashed line:* gray atmosphere; *dash-dot line:* colors and magnitude derived from a blackbody distribution.

the mass of the faintest objects is found to be less than 0.055 $M_\odot$, quite an unrealistic value for the objects presently considered.

The previous examinations clearly show that no fine age or metallicity determination for VLMSs with $M_V > 15$ can be done with the present magnitude-color diagram. The effect on the *color-color* diagram will be examined below. Also shown in Figure 2 are evolutionary tracks calculated with a blackbody distribution. This shows convincingly, as already pointed out by several authors, the total inadequacy of such an approximation for modeling stars with $M \lesssim 0.6\ M_\odot$.

3. TiO *and* H_2O *effect.*—A major source of absorption for VLMSs below ~ 3200 K is due to TiO, and to a smaller extent to VO, in the optical, and to H_2O in the infrared (see, e.g., Dorman et al. 1989). The "Base" models, based on a straight mean approximation, *over*estimate the opacities throughout the spectrum, which yields atmospheric temperatures that are artificially high. This explains the slight discrepancy between theory and observation for $M_V > 15$. Preliminary calculations based on the "NextGen" grid, which includes a more accurate line-by-line treatment, lead to models about 200 K cooler. This analysis is also supported by the excellent agreement between theory and observation for the metal-deficient subdwarf sequence, for which the observations reveal the near-absence of TiO and H_2O bands. That stresses the importance of an accurate treatment of the molecular opacities, in particular TiO and H_2O, in modeling accurately the thermal properties of VLMSs with solar-like metallicity.

4. *Treatment of the atmosphere.*—Figure 2 also displays calculations within the standard Eddington approximation $[T_{surf} = T_{eff} = T(\tau = \frac{2}{3})]$, using the Rosseland opacities of AF94, for [M/H] = 0 and $t = 10$ Gyr (*dashed line*). As expected, the Eddington approximation departs from the correct calculations above $M_V = 15$, which corresponds to $T_{eff} \sim 2800$ K and $M = 0.15\ M_\odot$, whereas it reproduces the results obtained with the "Base" models below this limit. At this temperature, the convective zone penetrates up to an optical depth $\tau \approx 0.05$. The maximum departure occurs at $T_{eff} = 3300$ K, where the Eddington approximation model is ~ 200 K too hot.

5. *Mass determination.*—This is certainly the most interesting characteristic, for it allows the unambiguous determination of a genuine brown dwarf. Table 1 gives the various parameters identification, for three metallicites, down to the brown dwarf domain. Note that our models reproduce the observationally determined masses, radii, and effective temperatures of the two eclipsing binary systems CM Dra ($M = 0.237$ and $0.207\ M_\odot$; $T_{eff} = 3150 \pm 100$ K; $M_{bol} = 10.39$ and 10.54 ± 0.11) (Lacy 1977) and YY Gem ($M = 0.62$ and $0.57\ M_\odot$; $T_{eff} = 3806$ and 3742 ± 200 K; $M_{bol} = 7.78$ and 8.13 ± 0.1) (Leung & Schneider 1978), within the observed error bars. More detailed calculations for these two particular objects are in progress (Chabrier & Baraffe 1995). As already mentioned, previous models predict effective temperatures that are too large (by about 200 K) over the VLMS mass range, and fail to reproduce CM Dra and YY Gem characteristics.

The faintest observed objects are found to have masses $\sim 0.085\ M_\odot$ for the [M/H] = 0 and [M/H] = −0.5 sequences, and $\sim 0.09\ M_\odot$ for the [M/H] = −1.5 sequence. All these masses lie above the HBMM. Because of the absence of grains in the "Base" models of AH95, we did not follow the evolution of lower masses into the brown dwarf domain. The lowest calculated masses, corresponding to the end of the theoretical tracks in Figure 1, are $M = 0.078\ M_\odot$ for [M/H] = 0 and $M = 0.085\ M_\odot$ for [M/H] = −1.5. These calculations suggest the simple linear magnitude-color relationship for $M_V > 15$ and [M/H] = 0 and −0.5: $M_V \approx 2.94(V-I) + 5.52$. This clearly differs from the turnaround suggested by Bessell (1991) and the present observations by Monet et al. (1992) and Kirkpatrick et al. (1993, 1994) based on the observation of the two objects LHS 2924 and LHS 2065. This suggests either a bias in the observations or a very peculiar behavior for the colors of the objects at the very bottom of the dwarf sequence. Such a

TABLE 1

M DWARF IDENTIFICATION[a]

[M/H]	M_V	M_{bol}	$(V-I)$	$(I-J)$	T_{eff}	$M/M_\odot$
0	9.58	7.71	2.26	1.39	3790	0.6
	10.76	8.49	2.54	1.61	3494	0.5
	11.70	9.18	2.70	1.74	3309	0.4
	12.52	9.82	2.82	1.83	3202	0.3
	13.69	10.70	3.00	1.98	3073	0.2
	14.67	11.35	3.20	2.15	2964	0.15
	17.12	12.56	3.88	2.82	2668	0.1
	18.51	13.07	4.35	3.30	2492	0.09
	21.50	14.00	5.41	4.37	2122	0.08
	22.37	14.27	5.74	4.64	2016	0.078
−0.5	10.33	8.75	2.11	1.22	3627	0.4
	11.41	9.55	2.32	1.35	3447	0.3
	12.57	10.43	2.53	1.47	3305	0.2
	13.55	11.10	2.75	1.60	3181	0.15
	15.92	12.32	3.51	2.12	2860	0.1
	17.30	12.84	4.02	2.54	2675	0.09
	20.51	13.88	5.18	3.70	2252	0.08
−1.5	11.02	9.92	1.73	0.99	3782	0.2
	11.89	10.64	1.86	1.05	3625	0.15
	13.64	11.92	2.29	1.25	3242	0.1
	14.68	12.52	2.67	1.41	3004	0.09
	15.97	13.10	3.28	1.64	2745	0.085

[a] The colors and magnitudes have been calculated with the standard Johnson-Cousins system for *VRI* and the CIT system for *JHK* (see AH95).

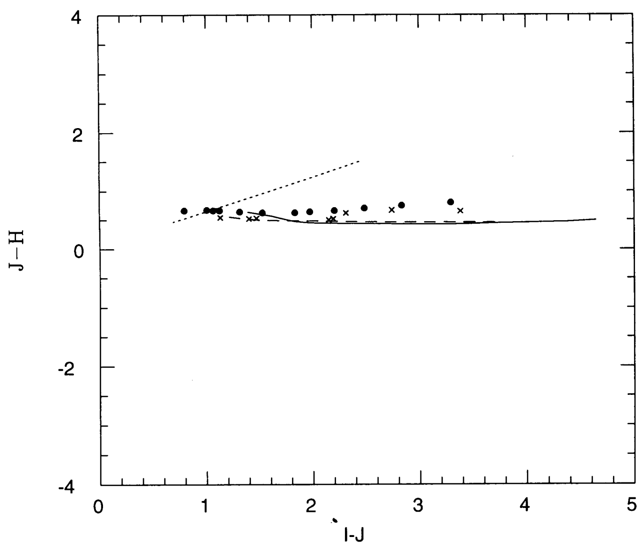

FIG. 3.—Color-color diagram. *Crosses:* Kirkpatrick et al. (1993, 1994); *filled circles:* Bessell (1991). All calculations are for $t = 10^{10}$ yr. *Solid line:* [M/H] = 0; *dashed line:* [M/H] = −0.5; *dotted line:* blackbody distribution.

particular effect might stem either from an inaccurate treatment of the opacity in the *V* or *I* band or from the onset of grain formation. Another exciting possibility would be that the two aforementioned objects are metal-depleted brown dwarfs, to be linked with the *subdwarf* sequence.

6. *Color-color diagram.*—As shown in Figure 3, the agreement between theory and observation in the *IJH* diagram is excellent. A similar comparison in $J-K$ shows an underestimation of ~0.4 mag in the theory for the reddest objects. This stems from the overestimated strengths of H_2O bands due to the straight mean approximation used by AH95, as clearly illustrated in Figure 10 of AH95 and discussed in Brett (1994). Masses can be identified in Table 1. Models with $t = 10^8$ yr are almost undistinguishable (but the masses are different!). That clearly shows that these colors are inadequate to determine the age or the metallicity of these objects.

3. CONCLUSION

In this Letter we have reported the first evolutionary calculations for cool M dwarfs, based on detailed model atmospheres at various metallicities. The calculations accurately reproduce the observational results, therefore assessing the validity of the present models to characterize low-mass and very low mass star structure and evolution. We identify the masses, metallicities, and effective temperatures of the two M dwarf sequences observed by Monet et al. (1992) and Kirkpatrick et al. (1993, 1994). The faintest observed objects are found to lie slightly above the hydrogen-burning minimum mass. The present calculations show the crucial importance of the treatment of the atmosphere, and of the molecular bands, in modeling accurately the evolution of these objects. The simple Eddington approximation is found to be quite unreliable over most of the corresponding mass range.

The present calculations do not show the color saturation effect shown by the observations of the two faintest objects, but rather display a simple linear magnitude-color relation. If such a color saturation effect is real, it suggests a peculiar behavior of the energy distribution at these temperatures. Another titillating hypothesis is that these objects are actually brown dwarfs. An investigation of these various possibilities is in progress.

The authors are very grateful to Dave Alexander for kindly providing his Rosseland opacities and to the anonymous referee for his useful comments and his corrections of the initial manuscript. This work was funded in part by grants to G. F. Fahlman and H. B. Richer from NSERC (Canada) and by a NASA LTSA grant to Arizona State University. Some of the calculations presented in this paper were performed on the Cray C90 of the San Diego Supercomputer Center (SDSC); we thank them for a generous allocation of computer time.

REFERENCES

Alexander, D. R., & Ferguson, J. W. 1994, ApJ, 437, 879 (AF94)
Allard, F. 1990, Ph.D. thesis, Univ. Heidelberg
Allard, F., & Hauschildt, P. H. 1995, ApJ, 445, 433 (AH95)
Auman, J. R. 1969, ApJ, 157, 799
Bessell, M. S. 1991, AJ, 101, 662
Brett, J. M. 1994, A&A, in press
Brett, J. M., & Plez, B. 1993, Proc. Astron. Soc. Australia, 10, 250
Burrows, A., Hubbard, W. B., Saumon, D., & Lunine, J. I. 1993, ApJ, 406, 158
Burrows, A., Hubbard, W. B., & Lunine, J. I. 1989, ApJ, 345, 939
Chabrier, G., & Baraffe, I. 1995, in preparation
Chabrier, G., Baraffe, I., & Plez, B. 1995, in preparation
D'Antona, F., & Mazzitelli, I. 1985, ApJ, 296, 502
———. 1994, ApJS, 90, 467
Dorman, B., Nelson, L. A., & Chau, W. Y. 1989, ApJ, 342, 1003
Kirkpatrick, J. D., Kelly, D. M., Tieke, G. H., Liebert, J., Allard, F., & Wehrse, R. 1993, ApJ, 402, 643
Kirkpatrick, J. D., McGraw, J. T., Hess, T. R., Liebert, J., & McCarthy, D. W., Jr. 1994, ApJS, 94, 749
Kui, R. 1991, Ph.D. thesis, National Univ. Australia
Lacy, C. H. 1977, ApJ, 218, 444
Leung, K.-C., & Schneider, D. 1978, AJ, 83, 618
Monet, D. G., Dahn, C. C., Vrba, F. J., Harris, H. C., Pier, J. R., Luginbuhl, C. B., & Ables, H. D. 1992, AJ, 103, 638
Nelson, L. A., Rappaport, S., & Joss, P. C. 1993, ApJ, 404, 723
Saumon, D., Bergeron, P., Lunine, L. I., Hubbard, W. B., & Burrows, A. 1994, ApJ, 424, 333
Saumon, D., & Chabrier, G. 1992, Phys. Rev. A, 46, 2084
Saumon, D., Chabrier, G., & Van Horn, H. M. 1995, ApJS, in press